

Cite this: DOI: 10.1039/xxxxxxxxxx

Supporting Information: A microfluidic strategy for the detection of membrane protein interactions[†]

Yuewen Zhang^{a,§,‡}, Therese W. Herling^{a,‡}, Stefan Kreida^b, Quentin A.E. Peter^a, Tadas Kartanas^a, Susanna Törnroth-Horsefield^b, Sara Linse^{*b}, Tuomas P.J. Knowles^{*a,c}

Received Date
Accepted Date

DOI: 10.1039/xxxxxxxxxx

www.rsc.org/journalname

Microfluidic diffusional sizing

A microfluidic diffusional sizing design with the measurement channel passing through the field of view four times was used in the present experiments (Fig. 1 and SI Fig. 1a). The channel is 300 μm wide, and profiles were collected at points 1 mm, 10 mm, 20 mm, and 40 mm along the diffusion channel.

CaM interacts with AQP0 to form a complex. Fractional contributions from the isolated (c) and bound protein (b) result in the observed diffusion coefficient (D_{obs}). Here, the observed species is labelled CaM and the total concentration of observed protein (c_t):

$$D_{obs} = D_c \cdot \frac{c}{c_t} + D_b \cdot \frac{c_t - c}{c_t} \quad (1)$$

The K_d for the interaction with the binding partner (a), can be expressed in terms of c and the total concentrations in the sample, c_t and a_t :

$$K_d = \frac{c \cdot a}{b} = \frac{c \cdot (a_t - c_t + c)}{c_t - c} \quad (2)$$

The expression (Eqn. 2) was solved for c , giving a quadratic equation with the solution¹

$$c = \frac{-a_t + c_t - K_d + \sqrt{(a_t - c_t + K_d)^2 + 4 \cdot K_d \cdot c_t}}{2} \quad (3)$$

Equations 1 and 3 were combined and used to fit the data

(SI Fig. 1b).

Depending on the method used, one or two CaM molecules have been reported to bind AQP0 with K_d values ranging from <100 nM to 40 μM .²⁻⁵ We were able to fit the data with a single binding site and K_d . However, the observed binding curves could also be compatible with the sequential cooperative binding of two CaM per AQP0 tetramer, as previously reported.⁵ In addition, we therefore investigated whether a model with the sequential binding of two CaM to each AQP0 tetramer with two K_d values (K_{d1} , K_{d2} would improve the fit to the data (SI Fig. 1c).

$$K_{d1} = \frac{c \cdot a}{ca} \quad (4)$$

$$K_{d2} = \frac{c \cdot ca}{c_2a} \quad (5)$$

Where the total CaM and AQP concentrations were

$$c_t = c + ca + 2 \cdot c_2a \quad (6)$$

$$a_t = a + ca + c_2a \quad (7)$$

Giving three potential states for CaM

$$D_{obs} = D_c \cdot \frac{c}{c_t} + D_{ca} \cdot \frac{ca}{c_t} + D_{c_2a} \cdot \frac{c_2a}{c_t} \quad (8)$$

The above equations were solved for c , the concentration of unbound CaM, and the data fitted with D_c , D_{ca} , D_{c_2a} , K_{d1} , and K_{d2} as fitting parameters (SI Fig. 1c). The inclusion of additional free parameters (the size of a complex with two CaM bound and a second K_d) did not improve the fit markedly. The resulting diffusion coefficients for one and two CaM bound corresponded to radii of 6.3 nm and 7.0 nm. We have therefore applied the simplest model that would describe the data in this study.

^a Department of Chemistry, University of Cambridge, Lensfield Road, Cambridge, CB2 1EW, UK. E-mail: tpjk2@cam.ac.uk

^b Department of Biochemistry and Structural Biology, Lund University, Lund, 221 00, Sweden.

^c Cavendish Laboratory, University of Cambridge, J J Thomson Avenue, Cambridge, CB3 0HE, UK.

[§] Current address: Department of Chemistry, Lanzhou University, Lanzhou, Gansu, 730000, P.R. China.

[‡] These authors contributed equally to this work.

[†] Electronic Supplementary Information (ESI) available: [details of any supplementary information available should be included here]. See DOI: 10.1039/b000000x/

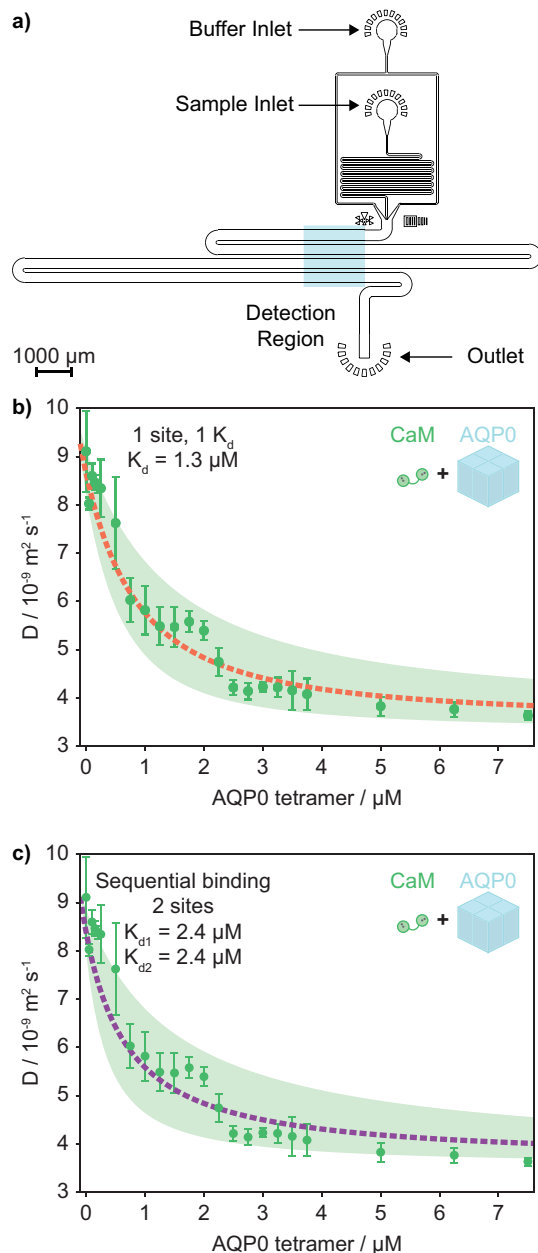


Fig. 1 (a) Schematic of the microfluidic device design used in this study. The channel passes through the detection region four times in order to collect data for diffusion at multiple time points within a single image. (b) Observed D for $1 \mu\text{M}$ CaM as a function of AQP0 concentration. Fitting the data with one binding site per tetramer results in a K_d of $1.3 \mu\text{M}$. (c) Fit to the diffusion data with two K_d values and two sequential binding events to allow for cooperativity gives $K_{d1} = 2.4 \mu\text{M}$ and $K_{d2} = 2.4 \mu\text{M}$. The shaded areas covers a factor 2 in the K_d values and the fitted diffusion coefficients \pm the mean percentage error on the measured D .

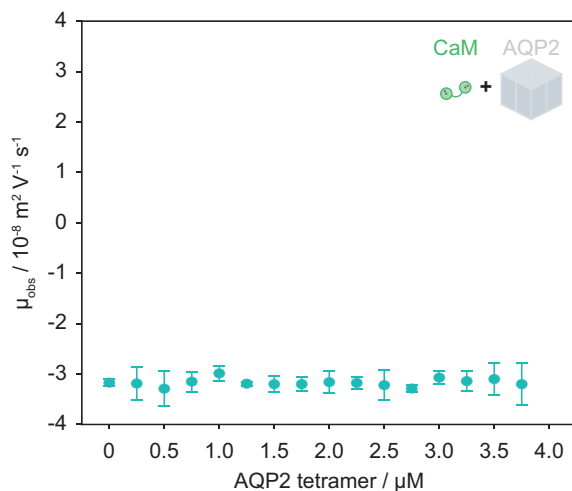


Fig. 2 The observed μ_{obs} of CaM against an increasing concentration of AQP2 tetramer. Errorbars represent the standard deviation of three independent measurement repeats for each sample concentration.

Microfluidic free flow electrophoresis

Microfluidic free flow electrophoresis was applied in the study of CaM binding to AQP isoforms, including AQP2. Unlike the interaction with AQP0, CaM did not show binding to AQP2 by either microfluidic diffusional sizing or free flow electrophoresis (Fig. 2b and SI Fig. 2).

In a similar manner to D_{obs} , the observed electrophoretic mobility reports on the fractional contributions from bound and isolated protein (Eqn. 9).

$$\mu_{\text{obs}} = \mu_c \cdot \frac{c}{c_t} + \mu_b \cdot \frac{c_t - c}{c_t} \quad (9)$$

In order to analyse the electrophoretic mobility change in response to complex formation, we employed an analogous approach to the analysis outlined above for the diffusional sizing data. The electrophoresis measurements were performed with either CaM or AQP0 in excess (Fig. 4 and SI Fig. 3). All data analysis was carried out using Python. We adapted the analysis script depending on which binding partner was observed (CaM-AlexaFluor488 or unlabelled AQP0). As in the case of the diffusional sizing data, we tested models with one binding site or two sequential binding events per AQP0 tetramer. The resulting μ_e values for one and two CaM bound were close (-0.28 and $-0.12 \times 10^{-8} \text{ m}^2 \text{ V}^{-1} \text{ s}^{-1}$ for CaM-AlexaFluor488, and -0.48 and $-0.49 \times 10^{-8} \text{ m}^2 \text{ V}^{-1} \text{ s}^{-1}$ for intrinsic AQP0 fluorescence).

The resulting K_d values indicated micromolar affinity with strong positive cooperativity. The data is thus compatible with two CaM molecules binding to each AQP0 tetramer. However, the inclusion of a second binding site and K_d value did not improve the fit markedly when comparing the residuals. The data for these experimental conditions does therefore not definitively show that two CaM bind AQP0 in low salt buffer.

The microfluidic measurements were performed in a buffer with relatively low salt content to minimise charge screening by solvent ions (10 mM Tris-HCl, 10 mM NaCl, 0.03% DDM, pH 7.5, with 0.1 mM CaCl₂). Calmodulin carries a considerable negative

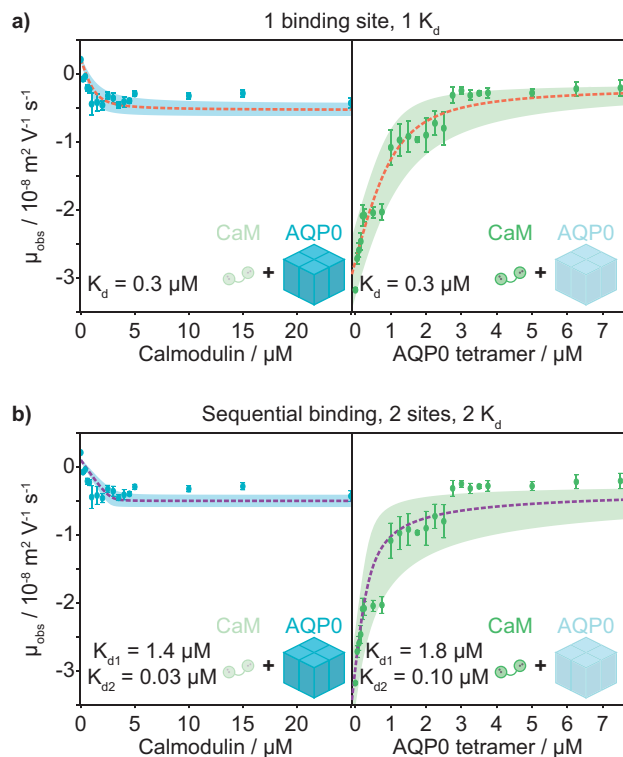


Fig. 3 (a) Data fits for 1 binding site per AQP0 tetramer. Left, the observed μ_{obs} for 1 μM CaM in the presence of increasing AQP0. Right, the observed μ_e for 1.25 μM AQP0 tetramer as a function of CaM concentration. (b) Data from (a) fitted to a model with sequential binding to two sites per AQP0 tetramer and two K_d values. The shaded areas covers a factor 2 in the K_d values and the fitted diffusion coefficients \pm the mean percentage error on the measured μ_{obs} .

charge (Fig. 4d), electrostatic repulsion between CaM molecules could therefore favour the binding of one rather than two CaM per tetramer. Previous studies of CaM binding to full-length AQP0 were performed at higher salt concentrations (20 mM Tris, pH 7.5, 100 mM NaCl, 1 mM CaCl₂, 5% glycerol, 0.05% DDM).⁵ Analysis of CaM binding to peptide ligands, found the target-affinity and Ca²⁺ binding to be affected by the salt concentration.^{6,7} Binding to full-length proteins and the number of binding sites used may therefore also be affected by the ionic strength.

In addition, we used the Adair equation as applied in previous studies to describe the electrophoretic mobility measurements for 1.25 μM AQP0 tetramer in the presence of increasing CaM, SI Fig. 4.⁵ The Adair equation with two binding sites also describes the data. The observed mobility is expressed as

$$\mu_{\text{obs}} = \mu_a \cdot \frac{(\mu_{\text{ac}} - \mu_a) \cdot K_{d1} \cdot c + (\mu_{\text{c2a}} - \mu_a) \cdot K_{d2} \cdot c^2}{1 + K_{d1} \cdot c + K_{d2} \cdot c^2} \quad (10)$$

Where μ_a is the electrophoretic mobility for unbound AQP0. The concentration of free CaM was isolated from

$$c_f = c + \frac{K_{d1} \cdot c + K_{d2} \cdot c^2}{1 + K_{d1} \cdot c + K_{d2} \cdot c^2} \quad (11)$$

In this case, we observed positive cooperativity with K_d val-

ues in the micromolar range, in line with previous findings and

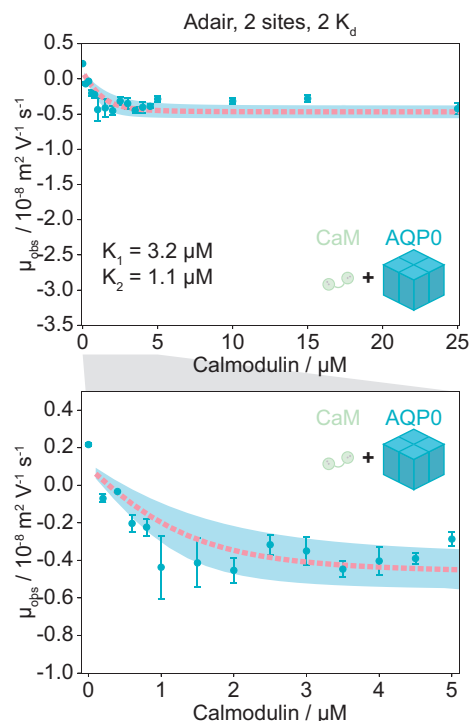


Fig. 4 (a) Using the Adair equation to fit the observed μ_{obs} for 1.25 μM AQP0 tetramer as a function of CaM concentration. (b) Zoom of 0–5 μM CaM in (a). The shaded areas covers a factor 2 in the K_d values and the fitted diffusion coefficients \pm the mean percentage error on the measured μ_{obs} .

the data analysis above.⁵ The fit to the data was not notably improved by the inclusion of additional free parameters relative to the 1:1 interaction. In the main text, we therefore describe the data using the simplest model of one CaM binding to each AQP0 tetramer.

References

- 1 T. W. Herling, D. J. O'Connell, M. C. Bauer, J. Persson, U. Weininger, T. P. J. Knowles and S. Linse, *Biophysical Journal*, 2016, **110**, 1957–1966.
- 2 S. L. Reichow and T. Gonen, *Structure*, 2008, **16**, 1389–1398.
- 3 K. M. L. Rose, Z. Wang, G. N. Magrath, E. S. Hazard, J. D. Hildebrandt and K. L. Schey, *Biochemistry*, 2008, **47**, 339–347.
- 4 S. L. Reichow, D. M. Clemens, J. A. Freites, K. L. Németh-Cahalan, M. Heyden, D. J. Tobias, J. E. Hall and T. Gonen, *Nature Structural & Molecular Biology*, 2013, **20**, 1085–1092.
- 5 S. Kreida, J. V. Roche, C. Olsson, S. Linse and S. Törnroth-Horsefield, *Faraday Discussions*, 2018, **209**, 35–54.
- 6 B. Svensson, B. Jonsson and E. Thulin, *Biochemistry*, 1993, **32**, 2828–2834.
- 7 I. André, T. Kesvatera, B. Jönsson and S. Linse, *Biophysical Journal*, 2006, **90**, 2903–2910.